

Search for New Hadronic Decays of h_c and Observation of $h_c \rightarrow K^+ K^- \pi^+ \pi^- \pi^0$

M. Ablikim¹, M. N. Achasov^{10,c}, P. Adlarson⁶⁷, S. Ahmed¹⁵, M. Albrecht⁴, R. Aliberti²⁸, A. Amoroso^{66A,66C}, M. R. An³², Q. An^{63,49}, X. H. Bai⁵⁷, Y. Bai⁴⁸, O. Bakina²⁹, R. Baldini Ferroli^{23A}, I. Balossino^{24A}, Y. Ban^{38,k}, K. Begzsuren²⁶, N. Berger²⁸, M. Bertani^{23A}, D. Bettoni^{24A}, F. Bianchi^{66A,66C}, J. Bloms⁶⁰, A. Bortone^{66A,66C}, I. Boyko²⁹, R. A. Briere⁵, H. Cai⁶⁸, X. Cai^{1,49}, A. Calcaterra^{23A}, G. F. Cao^{1,54}, N. Cao^{1,54}, S. A. Cetin^{53B}, J. F. Chang^{1,49}, W. L. Chang^{1,54}, G. Chelkov^{29,b}, D. Y. Chen⁶, G. Chen¹, H. S. Chen^{1,54}, M. L. Chen^{1,49}, S. J. Chen³⁵, X. R. Chen²⁵, Y. B. Chen^{1,49}, Z. J. Chen^{20,l}, W. S. Cheng^{66C}, G. Cibinetto^{24A}, F. Cossio^{66C}, X. F. Cui³⁶, H. L. Dai^{1,49}, X. C. Dai^{1,54}, A. Dbeyssi¹⁵, R. E. de Boer⁴, D. Dedovich²⁹, Z. Y. Deng¹, A. Denig²⁸, I. Denysenko²⁹, M. Destefanis^{66A,66C}, F. De Mori^{66A,66C}, Y. Ding³³, C. Dong³⁶, J. Dong^{1,49}, L. Y. Dong^{1,54}, M. Y. Dong^{1,49,54}, X. Dong⁶⁸, S. X. Du⁷¹, Y. L. Fan⁶⁸, J. Fang^{1,49}, S. S. Fang^{1,54}, Y. Fang¹, R. Farinelli^{24A}, L. Fava^{66B,66C}, F. Feldbauer⁴, G. Felici^{23A}, C. Q. Feng^{63,49}, J. H. Feng⁵⁰, M. Fritsch⁴, C. D. Fu¹, Y. Gao⁶⁴, Y. Gao^{38,k}, Y. Gao^{63,49}, Y. G. Gao⁶, I. Garzia^{24A,24B}, P. T. Ge⁶⁸, C. Geng⁵⁰, E. M. Gersabeck⁵⁸, K. Goetzen¹¹, L. Gong³³, W. X. Gong^{1,49}, W. Gradl²⁸, M. Greco^{66A,66C}, L. M. Gu³⁵, M. H. Gu^{1,49}, S. Gu², Y. T. Gu¹³, C. Y. Guan^{1,54}, A. Q. Guo²², L. B. Guo³⁴, R. P. Guo⁴⁰, Y. P. Guo^{9,h}, A. Guskov²⁹, T. T. Han⁴¹, W. Y. Han³², X. Q. Hao¹⁶, F. A. Harris⁵⁶, K. L. He^{1,54}, F. H. Heinsius⁴, C. H. Heinz²⁸, T. Held⁴, Y. K. Heng^{1,49,54}, C. Herold⁵¹, M. Himmelreich^{11,f}, T. Holtmann⁴, Y. R. Hou⁵⁴, Z. L. Hou¹, H. M. Hu^{1,54}, J. F. Hu^{47,m}, T. Hu^{1,49,54}, Y. Hu¹, G. S. Huang^{63,49}, L. Q. Huang⁶⁴, X. T. Huang⁴¹, Y. P. Huang¹, Z. Huang^{38,k}, N. Huesken⁶⁰, T. Hussain⁶⁵, W. Ikegami Andersson⁶⁷, W. Imoehl²², M. Irshad^{63,49}, S. Jaeger⁴, S. Janchiv^{26,j}, Q. Ji¹, Q. P. Ji¹⁶, X. B. Ji^{1,54}, X. L. Ji^{1,49}, H. B. Jiang⁴¹, X. S. Jiang^{1,49,54}, J. B. Jiao⁴¹, Z. Jiao¹⁸, S. Jin³⁵, Y. Jin⁵⁷, T. Johansson⁶⁷, N. Kalantar-Nayestanaki⁵⁵, X. S. Kang³³, R. Kappert⁵⁵, M. Kavatsyuk⁵⁵, B. C. Ke^{43,1}, I. K. Keshk⁴, A. Khokkaz⁶⁰, P. Kiese²⁸, R. Kiuchi¹, R. Kliemt¹¹, L. Koch³⁰, O. B. Kolcu^{53B,e}, B. Kopf⁴, M. Kuemmel⁴, M. Kuessner⁴, A. Kupsc⁶⁷, M. G. Kurth^{1,54}, W. Kühn³⁰, J. J. Lane⁵⁸, J. S. Lange³⁰, P. Larin¹⁵, A. Lavania²¹, L. Lavezzi^{66A,66C}, Z. H. Lei^{63,49}, H. Leithoff²⁸, M. Lellmann²⁸, T. Lenz²⁸, C. Li³⁹, C. H. Li³², Cheng Li^{63,49}, D. M. Li⁷¹, F. Li^{1,49}, G. Li¹, H. Li⁴³, H. Li^{63,49}, H. B. Li^{1,54}, H. J. Li^{9,h}, J. L. Li⁴¹, J. Q. Li⁴, J. S. Li⁵⁰, Ke Li¹, L. K. Li¹, Lei Li³, P. R. Li³¹, S. Y. Li⁵², W. D. Li^{1,54}, W. G. Li¹, X. H. Li^{63,49}, X. L. Li⁴¹, Z. Y. Li⁵⁰, H. Liang^{63,49}, H. Liang^{1,54}, H. Liang²⁷, Y. F. Liang⁴⁵, Y. T. Liang²⁵, L. Z. Liao^{1,54}, J. Libby²¹, C. X. Lin⁵⁰, B. J. Liu¹, C. X. Liu¹, D. Liu^{63,49}, F. H. Liu⁴⁴, Fang Liu¹, Feng Liu⁶, H. B. Liu¹³, H. M. Liu^{1,54}, Huanhuan Liu¹, Huihui Liu¹⁷, J. B. Liu^{63,49}, J. L. Liu⁶⁴, J. Y. Liu^{1,54}, K. Liu¹, K. Y. Liu³³, Ke Liu⁶, L. Liu^{63,49}, M. H. Liu^{9,h}, P. L. Liu¹, Q. Liu⁵⁴, Q. Liu⁶⁸, S. B. Liu^{63,49}, Shuai Liu⁴⁶, T. Liu^{1,54}, W. M. Liu^{63,49}, X. Liu³¹, Y. Liu³¹, Y. B. Liu³⁶, Z. A. Liu^{1,49,54}, Z. Q. Liu⁴¹, X. C. Lou^{1,49,54}, F. X. Lu⁵⁰, F. X. Lu¹⁶, H. J. Lu¹⁸, J. D. Lu^{1,54}, J. G. Lu^{1,49}, X. L. Lu¹, Y. Lu¹, Y. P. Lu^{1,49}, C. L. Luo³⁴, M. X. Luo⁷⁰, P. W. Luo⁵⁰, T. Luo^{9,h}, X. L. Luo^{1,49}, S. Lusso^{66C}, X. R. Lyu⁵⁴, F. C. Ma³³, H. L. Ma¹, L. L. Ma⁴¹, M. M. Ma^{1,54}, Q. M. Ma¹, R. Q. Ma^{1,54}, R. T. Ma⁵⁴, X. X. Ma^{1,54}, X. Y. Ma^{1,49}, F. E. Maas¹⁵, M. Maggiora^{66A,66C}, S. Maldaner⁴, S. Malde⁶¹, Q. A. Malik⁶⁵, A. Mangoni^{23B}, Y. J. Mao^{38,k}, Z. P. Mao¹, S. Marcello^{66A,66C}, Z. X. Meng⁵⁷, J. G. Messchendorp⁵⁵, G. Mezzadri^{24A}, T. J. Min³⁵, R. E. Mitchell²², X. H. Mo^{1,49,54}, Y. J. Mo⁶, N. Yu. Muchnoi^{10,c}, H. Muramatsu⁵⁹, S. Nakhoul^{11,f}, Y. Nefedov²⁹, F. Nerling^{11,f}, I. B. Nikolaev^{10,c}, Z. Ning^{1,49}, S. Nisar^{8,i}, S. L. Olsen⁵⁴, Q. Ouyang^{1,49,54}, S. Pacetti^{23B,23C}, X. Pan^{9,h}, Y. Pan⁵⁸, A. Pathak¹, P. Patteri^{23A}, M. Pelizaeus⁴, H. P. Peng^{63,49}, K. Peters^{11,f}, J. Pettersson⁶⁷, J. L. Ping³⁴, R. G. Ping^{1,54}, R. Poling⁵⁹, V. Prasad^{63,49}, H. Qi^{63,49}, H. R. Qi⁵², K. H. Qi²⁵, M. Qi³⁵, T. Y. Qi⁹, T. Y. Qi², S. Qian^{1,49}, W.-B. Qian⁵⁴, Z. Qian⁵⁰, C. F. Qiao⁵⁴, L. Q. Qin¹², X. S. Qin⁴, Z. H. Qin^{1,49}, J. F. Qiu¹, S. Q. Qu³⁶, K. H. Rashid⁶⁵, K. Ravindran²¹, C. F. Redmer²⁸, A. Rivetti^{66C}, V. Rodin⁵⁵, M. Rolo^{66C}, G. Rong^{1,54}, Ch. Rosner¹⁵, M. Rump⁶⁰, H. S. Sang⁶³, A. Sarantsev^{29,d}, Y. Schelhaas²⁸, C. Schnier⁴, K. Schoenning⁶⁷, M. Scodeggio^{24A,24B}, D. C. Shan⁴⁶, W. Shan¹⁹, X. Y. Shan^{63,49}, J. F. Shangguan⁴⁶, M. Shao^{63,49}, C. P. Shen⁹, P. X. Shen³⁶, X. Y. Shen^{1,54}, H. C. Shi^{63,49}, R. S. Shi^{1,54}, X. Shi^{1,49}, X. D. Shi^{63,49}, W. M. Song^{27,1}, Y. X. Song^{38,k}, S. Sosio^{66A,66C}, S. Spataro^{66A,66C}, K. X. Su⁶⁸, P. P. Su⁴⁶, F. F. Sui⁴¹, G. X. Sun¹, H. K. Sun¹, J. F. Sun¹⁶, L. Sun⁶⁸, S. S. Sun^{1,54}, T. Sun^{1,54}, W. Y. Sun²⁷, W. Y. Sun³⁴, X. Sun^{20,l}, Y. J. Sun^{63,49}, Y. K. Sun^{63,49}, Y. Z. Sun¹, Z. T. Sun¹, Y. H. Tan⁶⁸, Y. X. Tan^{63,49}, C. J. Tang⁴⁵, G. Y. Tang¹, J. Tang⁵⁰, J. X. Teng^{63,49}, V. Thoren⁶⁷, I. Uman^{53D}, C. W. Wang³⁵, D. Y. Wang^{38,k}, H. J. Wang³¹, H. P. Wang^{1,54}, K. Wang^{1,49}, L. L. Wang¹, M. Wang⁴¹, M. Z. Wang^{38,k}, Meng Wang^{1,54}, W. Wang⁵⁰, W. H. Wang⁶⁸, W. P. Wang^{63,49}, X. Wang^{38,k}, X. F. Wang³¹, X. L. Wang^{9,h}, Y. Wang^{63,49}, Y. Wang⁵⁰, Y. D. Wang³⁷, Y. F. Wang^{1,49,54}, Y. Q. Wang¹, Y. Y. Wang³¹, Z. Wang^{1,49}, Z. Y. Wang¹, Ziyi Wang⁵⁴, Zongyuan Wang^{1,54}, D. H. Wei¹², P. Weidenkaft²⁸, F. Weidner⁶⁰, S. P. Wen¹, D. J. White⁵⁸, U. Wiedner⁴, G. Wilkinson⁶¹, M. Wolke⁶⁷, L. Wollenberg⁴, J. F. Wu^{1,54}, L. H. Wu¹, L. J. Wu^{1,54}, X. Wu^{9,h}, Z. Wu^{1,49}, L. Xia^{63,49}, H. Xiao^{9,h}, S. Y. Xiao¹, Z. J. Xiao³⁴, X. H. Xie^{38,k}, Y. G. Xie^{1,49}, Y. H. Xie⁶, T. Y. Xing^{1,54}, G. F. Xu¹, Q. J. Xu¹⁴, W. Xu^{1,54}, X. P. Xu⁴⁶, F. Yan^{9,h}, L. Yan^{9,h}, W. B. Yan^{63,49}, W. C. Yan⁷¹, Xu Yan⁴⁶, H. J. Yang^{42,g}, H. X. Yang¹, L. Yang⁴³, S. L. Yang⁵⁴, Y. X. Yang¹², Yifan Yang^{1,54}, Zhi Yang²⁵, M. Ye^{1,49}, M. H. Ye⁷, J. H. Yin¹, Z. Y. You⁵⁰, B. X. Yu^{1,49,54}, C. X. Yu³⁶, G. Yu^{1,54}, J. S. Yu^{20,l}, T. Yu⁶⁴, C. Z. Yuan^{1,54}, L. Yuan², X. Q. Yuan^{38,k}, Y. Yuan¹, Z. Y. Yuan⁵⁰, C. X. Yue³², A. Yuncu^{53B,a}, A. A. Zafar⁶⁵, Y. Zeng^{20,l}, B. X. Zhang¹, Guangyi Zhang¹⁶, H. Zhang⁶³, H. H. Zhang⁵⁰, H. H. Zhang²⁷, H. Y. Zhang^{1,49}, J. J. Zhang⁴³, J. L. Zhang⁶⁹, J. Q. Zhang³⁴, J. W. Zhang^{1,49,54}, J. Y. Zhang¹, J. Z. Zhang^{1,54},

Jianyu Zhang^{1,54}, Jiawei Zhang^{1,54}, L. Q. Zhang⁵⁰, Lei Zhang³⁵, S. Zhang⁵⁰, S. F. Zhang³⁵, Shulei Zhang^{20,l}, X. D. Zhang³⁷, X. Y. Zhang⁴¹, Y. Zhang⁶¹, Y. H. Zhang^{1,49}, Y. T. Zhang^{63,49}, Yan Zhang^{63,49}, Yao Zhang¹, Yi Zhang^{9,h}, Z. H. Zhang⁶, Z. Y. Zhang⁶⁸, G. Zhao¹, J. Zhao³², J. Y. Zhao^{1,54}, J. Z. Zhao^{1,49}, Lei Zhao^{63,49}, Ling Zhao¹, M. G. Zhao³⁶, Q. Zhao¹, S. J. Zhao⁷¹, Y. B. Zhao^{1,49}, Y. X. Zhao²⁵, Z. G. Zhao^{63,49}, A. Zhemchugov^{29,b}, B. Zheng⁶⁴, J. P. Zheng^{1,49}, Y. Zheng^{38,k}, Y. H. Zheng⁵⁴, B. Zhong³⁴, C. Zhong⁶⁴, L. P. Zhou^{1,54}, Q. Zhou^{1,54}, X. Zhou⁶⁸, X. K. Zhou⁵⁴, X. R. Zhou^{63,49}, A. N. Zhu^{1,54}, J. Zhu³⁶, K. Zhu¹, K. J. Zhu^{1,49,54}, S. H. Zhu⁶², T. J. Zhu⁶⁹, W. J. Zhu³⁶, W. J. Zhu^{9,h}, X. L. Zhu⁵², Y. C. Zhu^{63,49}, Z. A. Zhu^{1,54}, B. S. Zou¹, J. H. Zou¹

(BESIII Collaboration)

- ¹ *Institute of High Energy Physics, Beijing 100049, People's Republic of China*
- ² *Beihang University, Beijing 100191, People's Republic of China*
- ³ *Beijing Institute of Petrochemical Technology, Beijing 102617, People's Republic of China*
- ⁴ *Bochum Ruhr-University, D-44780 Bochum, Germany*
- ⁵ *Carnegie Mellon University, Pittsburgh, Pennsylvania 15213, USA*
- ⁶ *Central China Normal University, Wuhan 430079, People's Republic of China*
- ⁷ *China Center of Advanced Science and Technology, Beijing 100190, People's Republic of China*
- ⁸ *COMSATS University Islamabad, Lahore Campus, Defence Road, Off Raiwind Road, 54000 Lahore, Pakistan*
- ⁹ *Fudan University, Shanghai 200443, People's Republic of China*
- ¹⁰ *G.I. Budker Institute of Nuclear Physics SB RAS (BINP), Novosibirsk 630090, Russia*
- ¹¹ *GSF Helmholtzcentre for Heavy Ion Research GmbH, D-64291 Darmstadt, Germany*
- ¹² *Guangxi Normal University, Guilin 541004, People's Republic of China*
- ¹³ *Guangxi University, Nanning 530004, People's Republic of China*
- ¹⁴ *Hangzhou Normal University, Hangzhou 310036, People's Republic of China*
- ¹⁵ *Helmholtz Institute Mainz, Johann-Joachim-Becher-Weg 45, D-55099 Mainz, Germany*
- ¹⁶ *Henan Normal University, Xinxiang 453007, People's Republic of China*
- ¹⁷ *Henan University of Science and Technology, Luoyang 471003, People's Republic of China*
- ¹⁸ *Huangshan College, Huangshan 245000, People's Republic of China*
- ¹⁹ *Hunan Normal University, Changsha 410081, People's Republic of China*
- ²⁰ *Hunan University, Changsha 410082, People's Republic of China*
- ²¹ *Indian Institute of Technology Madras, Chennai 600036, India*
- ²² *Indiana University, Bloomington, Indiana 47405, USA*
- ²³ *INFN Laboratori Nazionali di Frascati, (A)INFN Laboratori Nazionali di Frascati, I-00044, Frascati, Italy; (B)INFN Sezione di Perugia, I-06100, Perugia, Italy*
- ²⁴ *INFN Sezione di Ferrara, INFN Sezione di Ferrara, I-44122, Ferrara, Italy*
- ²⁵ *Institute of Modern Physics, Lanzhou 730000, People's Republic of China*
- ²⁶ *Institute of Physics and Technology, Peace Ave. 54B, Ulaanbaatar 13330, Mongolia*
- ²⁷ *Jilin University, Changchun 130012, People's Republic of China*
- ²⁸ *Johannes Gutenberg University of Mainz, Johann-Joachim-Becher-Weg 45, D-55099 Mainz, Germany*
- ²⁹ *Joint Institute for Nuclear Research, 141980 Dubna, Moscow region, Russia*
- ³⁰ *Justus-Liebig-Universitaet Giessen, II. Physikalisches Institut, Heinrich-Buff-Ring 16, D-35392 Giessen, Germany*
- ³¹ *Lanzhou University, Lanzhou 730000, People's Republic of China*
- ³² *Liaoning Normal University, Dalian 116029, People's Republic of China*
- ³³ *Liaoning University, Shenyang 110036, People's Republic of China*
- ³⁴ *Nanjing Normal University, Nanjing 210023, People's Republic of China*
- ³⁵ *Nanjing University, Nanjing 210093, People's Republic of China*
- ³⁶ *Nankai University, Tianjin 300071, People's Republic of China*
- ³⁷ *North China Electric Power University, Beijing 102206, People's Republic of China*
- ³⁸ *Peking University, Beijing 100871, People's Republic of China*
- ³⁹ *Qufu Normal University, Qufu 273165, People's Republic of China*
- ⁴⁰ *Shandong Normal University, Jinan 250014, People's Republic of China*
- ⁴¹ *Shandong University, Jinan 250100, People's Republic of China*
- ⁴² *Shanghai Jiao Tong University, Shanghai 200240, People's Republic of China*
- ⁴³ *Shanxi Normal University, Linfen 041004, People's Republic of China*
- ⁴⁴ *Shanxi University, Taiyuan 030006, People's Republic of China*
- ⁴⁵ *Sichuan University, Chengdu 610064, People's Republic of China*
- ⁴⁶ *Soochow University, Suzhou 215006, People's Republic of China*
- ⁴⁷ *South China Normal University, Guangzhou 510006, People's Republic of China*

- ⁴⁸ Southeast University, Nanjing 211100, People's Republic of China
- ⁴⁹ State Key Laboratory of Particle Detection and Electronics, Beijing 100049, Hefei 230026, People's Republic of China
- ⁵⁰ Sun Yat-Sen University, Guangzhou 510275, People's Republic of China
- ⁵¹ Suranaree University of Technology, University Avenue 111, Nakhon Ratchasima 30000, Thailand
- ⁵² Tsinghua University, Beijing 100084, People's Republic of China
- ⁵³ Turkish Accelerator Center Particle Factory Group, (A) Istanbul Bilgi University, 34060 Eyup, Istanbul, Turkey; (B) Near East University, Nicosia, North Cyprus, Mersin 10, Turkey
- ⁵⁴ University of Chinese Academy of Sciences, Beijing 100049, People's Republic of China
- ⁵⁵ University of Groningen, NL-9747 AA Groningen, The Netherlands
- ⁵⁶ University of Hawaii, Honolulu, Hawaii 96822, USA
- ⁵⁷ University of Jinan, Jinan 250022, People's Republic of China
- ⁵⁸ University of Manchester, Oxford Road, Manchester, M13 9PL, United Kingdom
- ⁵⁹ University of Minnesota, Minneapolis, Minnesota 55455, USA
- ⁶⁰ University of Muenster, Wilhelm-Klemm-Str. 9, 48149 Muenster, Germany
- ⁶¹ University of Oxford, Keble Rd, Oxford, UK OX13RH
- ⁶² University of Science and Technology Liaoning, Anshan 114051, People's Republic of China
- ⁶³ University of Science and Technology of China, Hefei 230026, People's Republic of China
- ⁶⁴ University of South China, Hengyang 421001, People's Republic of China
- ⁶⁵ University of the Punjab, Lahore-54590, Pakistan
- ⁶⁶ University of Turin and INFN, INFN, I-10125, Turin, Italy
- ⁶⁷ Uppsala University, Box 516, SE-75120 Uppsala, Sweden
- ⁶⁸ Wuhan University, Wuhan 430072, People's Republic of China
- ⁶⁹ Xinyang Normal University, Xinyang 464000, People's Republic of China
- ⁷⁰ Zhejiang University, Hangzhou 310027, People's Republic of China
- ⁷¹ Zhengzhou University, Zhengzhou 450001, People's Republic of China
- ^a Also at Bogazici University, 34342 Istanbul, Turkey
- ^b Also at the Moscow Institute of Physics and Technology, Moscow 141700, Russia
- ^c Also at the Novosibirsk State University, Novosibirsk, 630090, Russia
- ^d Also at the NRC "Kurchatov Institute", PNPI, 188300, Gatchina, Russia
- ^e Also at Istanbul Arel University, 34295 Istanbul, Turkey
- ^f Also at Goethe University Frankfurt, 60323 Frankfurt am Main, Germany
- ^g Also at Key Laboratory for Particle Physics, Astrophysics and Cosmology, Ministry of Education; Shanghai Key Laboratory for Particle Physics and Cosmology; Institute of Nuclear and Particle Physics, Shanghai 200240, People's Republic of China
- ^h Also at Key Laboratory of Nuclear Physics and Ion-beam Application (MOE) and Institute of Modern Physics, Fudan University, Shanghai 200443, People's Republic of China
- ⁱ Also at Harvard University, Department of Physics, Cambridge, MA, 02138, USA
- ^j Currently at: Institute of Physics and Technology, Peace Ave.54B, Ulaanbaatar 13330, Mongolia
- ^k Also at State Key Laboratory of Nuclear Physics and Technology, Peking University, Beijing 100871, People's Republic of China
- ^l School of Physics and Electronics, Hunan University, Changsha 410082, China
- ^m Also at Guangdong Provincial Key Laboratory of Nuclear Science, Institute of Quantum Matter, South China Normal University, Guangzhou 510006, China

(Dated: November 18, 2021)

Ten hadronic final states of the h_c decays are investigated via the process $\psi(3686) \rightarrow \pi^0 h_c$, using a data sample of $(448.1 \pm 2.9) \times 10^6$ $\psi(3686)$ events collected with the BESIII detector. The decay channel $h_c \rightarrow K^+ K^- \pi^+ \pi^- \pi^0$ is observed for the first time with a significance of 6.0σ . The corresponding branching fraction is determined to be $\mathcal{B}(h_c \rightarrow K^+ K^- \pi^+ \pi^- \pi^0) = (3.3 \pm 0.6 \pm 0.6) \times 10^{-3}$ (the first uncertainty is statistical and the second systematical). Evidence for the decays $h_c \rightarrow \pi^+ \pi^- \pi^0 \eta$ and $h_c \rightarrow K_S^0 K^\pm \pi^\mp \pi^+ \pi^-$ is found with a significance of 3.6σ and 3.8σ , respectively. The corresponding branching fractions (and upper limits) are obtained to be $\mathcal{B}(h_c \rightarrow \pi^+ \pi^- \pi^0 \eta) = (7.2 \pm 1.8 \pm 1.3) \times 10^{-3}$ ($< 1.8 \times 10^{-2}$) and $\mathcal{B}(h_c \rightarrow K_S^0 K^\pm \pi^\mp \pi^+ \pi^-) = (2.8 \pm 0.9 \pm 0.5) \times 10^{-3}$ ($< 4.7 \times 10^{-3}$). Upper limits on the branching fractions for the final states $h_c \rightarrow K^+ K^- \pi^0$, $K^+ K^- \eta$, $K^+ K^- \pi^+ \pi^- \eta$, $2(K^+ K^-) \pi^0$, $K^+ K^- \pi^0 \eta$, $K_S^0 K^\pm \pi^\mp$, and $p\bar{p} \pi^0 \pi^0$ are determined at a confidence level of 90%.

I. Introduction

Although the charmonium spectrum below the open-charm threshold seems to be well understood, it still gen-

erates unanswered questions. This is because the char-

monium states are located in the transition region of perturbative and non-perturbative quantum chromodynamics (QCD) and theoretical predictions suffer therefore from large uncertainties [1–4]. The study of charmonium states and their decays is therefore crucial for gaining a deeper understanding of the intermediate-energy regime of QCD, while QCD has been tested successfully at high energies [5]. For the h_c , χ_{cJ} and $\eta_c(2S)$ states, most of the decay channels are still unknown. After the discovery of the spin-singlet charmonium state $h_c(^1P_1)$ in 2005 [6, 7], there were only few measurements of its decays. Contrary to the fact that $h_c \rightarrow \gamma\eta_c$ is the prominent decay channel in every calculation, the predictions of the decay process $h_c \rightarrow \text{light hadrons}$ range from 14 – 48% [1–4] depending on the theoretical model. Therefore experimental measurements are needed to test and improve the theoretical models.

Experimental challenges arise from the limited statistics since these non-vector states cannot be produced directly in e^+e^- annihilation. The best-measured decay mode is the radiative transition $h_c \rightarrow \gamma\eta_c$, occurring in 51% of all decays [8–10], while the sum of all other known branching fractions is less than 3% [11]. Among these measurements, the multi-pionic decay $h_c \rightarrow 2(\pi^+\pi^-)\pi^0$ has been confirmed recently by the BESIII collaboration [12] after the first evidence was reported by CLEO-c [13]. Furthermore, BESIII observed the decay mode $h_c \rightarrow p\bar{p}\pi^+\pi^-$ and reported evidence for the decay $h_c \rightarrow \pi^+\pi^-\pi^0$. Since the previous analyses mainly studied multi-pionic final states, this analysis focuses on hadronic final states containing kaons as they could lead to intermediate resonances such as e.g. ϕ and excited kaon states. After radiative decays of the h_c to $\eta^{(\prime)}$ have been observed, the study of decays involving light vector-states different from the photon will be an extension of these observations. Finally, the observation of $h_c \rightarrow p\bar{p}\pi^+\pi^-$ motivated us to study the decay with neutral pions, as it could give additional hints on baryonic intermediate states.

From these considerations, the following ten final states are chosen to search for undiscovered decay channels of the h_c : (i) $h_c \rightarrow K^+K^-\pi^+\pi^-\pi^0$, (ii) $h_c \rightarrow \pi^+\pi^-\pi^0\eta$, (iii) $h_c \rightarrow K_S^0K^\pm\pi^\mp\pi^+\pi^-$, (iv) $h_c \rightarrow K^+K^-\pi^0$, (v) $h_c \rightarrow K^+K^-\eta$, (vi) $h_c \rightarrow K^+K^-\pi^+\pi^-\eta$, (vii) $h_c \rightarrow 2(K^+K^-\pi^0)$, (viii) $h_c \rightarrow K^+K^-\pi^0\eta$, (ix) $h_c \rightarrow K_S^0K^\pm\pi^\mp$, and (x) $h_c \rightarrow p\bar{p}\pi^0\pi^0$. These are referenced in this manuscript by roman numbers (i, ii, ..., x). In this analysis the h_c meson is produced via $\psi(3686) \rightarrow \pi^0 h_c$ using a data sample of $(448.1 \pm 2.9) \times 10^6$ $\psi(3686)$ events [14] collected with the BESIII detector.

II. BESIII Detector and Monte Carlo Simulation

The BESIII detector is a magnetic spectrometer [15] located at the Beijing Electron Positron Collider (BEPCII) [16]. The cylindrical core of the BESIII detector consists of a helium-based multilayer drift chamber (MDC), a plastic scintillator time-of-flight system (TOF), and a CsI(Tl) electromagnetic calorime-

ter (EMC), which are all enclosed in a superconducting solenoidal magnet providing a 1.0 T magnetic field. The solenoid is supported by an octagonal flux-return yoke with resistive plate counter muon identifier modules interleaved with steel. The acceptance of charged particles and photons is 93% over the 4π solid angle. The charged-particle momentum resolution at 1 GeV/c is 0.5%, and the dE/dx resolution is 6% for the electrons from Bhabha scattering. The EMC measures photon energies with a resolution of 2.5% (5%) at 1 GeV in the barrel (end cap) region. The time resolution of the TOF barrel part is 68 ps, while that of the end cap part is 110 ps.

GEANT4-based [17, 18] Monte Carlo (MC) simulations are used to study the detector response and to estimate background contributions. Inclusive MC samples are produced to estimate the contributions from possible background channels. The production of the initial $\psi(3686)$ resonance in e^+e^- annihilation is simulated using the MC event generator KKMC [19, 20]. Its known decay modes are modeled with EVTGEN [17, 18] using the world average branching fraction values [21], while the remaining unknown decays are generated using LUNDCHARM [22]. GEANT4 is used to simulate the particle propagation through the detector system. The simulation includes the beam-energy spread and initial-state radiation (ISR) in the e^+e^- annihilations. In addition, exclusive MC samples containing one million events are generated using the phase-space model (PHSP) for each signal mode to optimize the selection criteria and to study the efficiency.

III. Data Analysis

Each charged track reconstructed in the MDC is required to originate from a region of 10 cm of the interaction point along the beam direction and 1 cm in the plane perpendicular to the beam. The polar angle θ of the tracks must be within the fiducial volume of the MDC $|\cos\theta| < 0.93$. Tracks used in reconstructing K_S^0 mesons are exempted from these requirements and $|\cos\theta| < 0.93$ is required only for the daughter pions. The TOF and dE/dx measurements for each charged track are combined to compute particle identification (PID) confidence levels for pion, kaon and proton hypotheses. The track is assigned to the particle type with the highest confidence level which has to be larger than 0.001.

Photon candidates are reconstructed from electromagnetic showers produced in the crystals of the EMC. A shower is treated as a photon candidate if the deposited energy is larger than 25 MeV in the barrel region ($|\cos\theta| < 0.8$) or 50 MeV in the end cap region ($0.86 < |\cos\theta| < 0.92$). The timing of the shower is required to be within 700 ns from the reconstructed event start time to suppress noise and energy deposits unrelated to the event. To remove Bremsstrahlung photons, the angle between the photon and the extrapolated impact point in the EMC of the nearest charged track must be larger than 10° for charged pions and kaons and 20° for protons, respectively.

Following the application of a vertex fit that con-

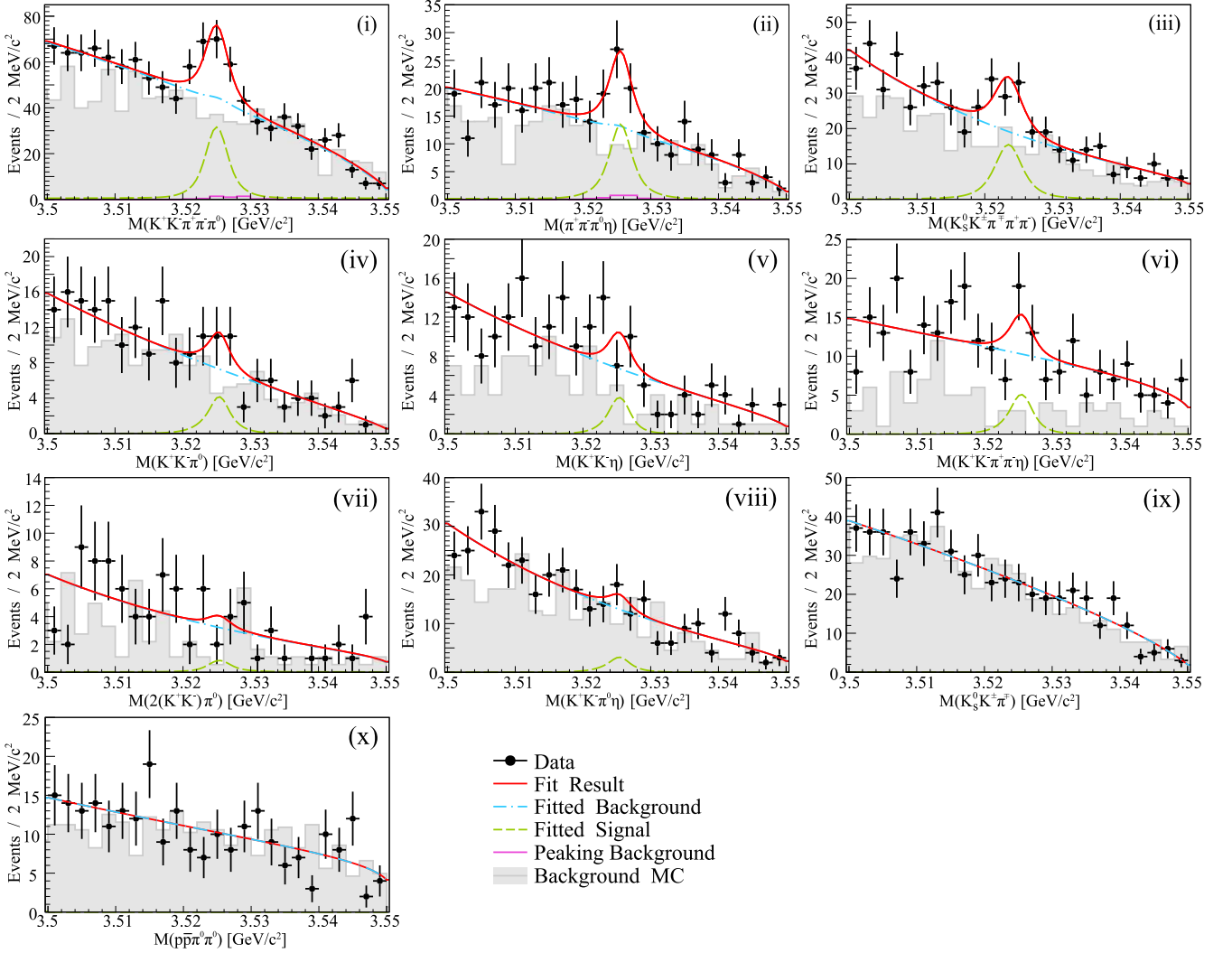


Figure 1. Fits to the invariant mass distributions for the h_c decay modes (i)-(x). Data are shown as black points, the total fit result is shown in red, the background contribution is denoted by the blue dashed-dotted line (including peaking background contributions for channel (i) and (ii) as shown in magenta), the signal contribution is illustrated by the green dashed line. The background level obtained from inclusive MC is shown by the gray shaded histogram.

straints all charged tracks to arise from a common interaction point, a kinematic fit, constraining the total energy and momentum to the initial four momentum, is performed to further improve the momentum resolution and to suppress background. Final states containing a K_S^0 undergo a secondary vertex fit, which ensures the daughter pions being produced in a common vertex. A K_S^0 candidate is accepted if $487 < M(\pi^+\pi^-) < 511 \text{ MeV}/c^2$ and $\lambda/\Delta\lambda > 2$, where $\Delta\lambda$ is the uncertainty on the decay length λ obtained from the secondary vertex fit.

A pair of photons is treated as a π^0 or η candidate if it satisfies $|M(\gamma\gamma) - M_{\pi^0}| < 30 \text{ MeV}/c^2$ or $|M(\gamma\gamma) - M_\eta| < 50 \text{ MeV}/c^2$, which corresponds to an interval of about ± 3 times the mass resolution. In all final states containing π^0 or η mesons, the kinematic fit also constraints $\gamma\gamma$ pairs

to have the expected nominal masses. The combination with the best χ^2 value is kept for the further analysis in case there are more than one $\gamma\gamma$ combinations.

To suppress contamination from decays with different numbers of photons, such as the dominant decay $\psi(3686) \rightarrow \gamma\chi_{c2}$, where the χ_{c2} decays to the same final states as the h_c , the following procedure is applied. The $\chi_{4C,n\gamma}^2$ value is obtained from a four-constraint fit including the expected number of photons n for a given signal hypothesis with respect to the initial four momentum. The value $\chi_{4C,(n-1)\gamma}^2$ is determined from an additional 4C fit with one missing photon compared to the desired signal process. An event is rejected if $\chi_{4C,n\gamma}^2 > \chi_{4C,(n-1)\gamma}^2$. To further suppress background, the $\chi_{(4+N)C}^2$ value of the total kinematic fit, including additional mass constraints for π^0 , η and K_S^0 candidates

Table I. Applied requirements on the $\chi^2_{(4+N)C}$ and mass windows used as vetoes in each exclusive mode. The lower case m denotes the nominal particle mass [11].

Mode	$\chi^2_{(4+N)C}$ limit	Mass Windows [MeV/ c^2]
(i)	< 60	$ M(\pi^+\pi^-)_{rec} - m_{J/\psi} > 25$ $ M(\pi^0\pi^0)_{rec} - m_{J/\psi} > 25$ $ M(\pi^+\pi^-\pi_1^0) - m_\omega > 20$ $ M(\pi^+\pi^-\pi_1^0) - m_\eta > 16$ $820 < M(K^\pm\pi_1^0) < 920$
(ii)	< 100	$ M(\pi^+\pi^-)_{rec} - m_{J/\psi} > 30$ $ M(\eta)_{rec} - m_{J/\psi} > 30$ $ M(\pi^+\pi^-\pi_1^0) - m_\omega > 20$ $ M(\pi^+\pi^-\pi_1^0) - m_\eta > 16$
(iii)	< 40	$ M(\pi^+\pi^-)_{rec} - m_{J/\psi} > 30$ $ M(\pi^+\pi^-\pi_1^0) - m_\omega > 20$ $ M(\pi^+\pi^-\pi_1^0) - m_\eta > 20$ $ M(K_S^0\pi_1^0) - m_{K^*} > 50$ $ M(K^\pm\pi_1^0) - m_{K^*} > 50$
(iv)	< 100	$ M(\pi^0\pi^0)_{rec} - m_{J/\psi} > 30$ $ M(K^\pm\pi_1^0) - m_{K^*} > 50$
(v)	< 100	
(vi)	< 60	$ M(\pi^+\pi^-)_{rec} - m_{J/\psi} > 30$ $ M(\eta)_{rec} - m_{J/\psi} > 30$ $ M(K^\pm\pi_1^0) - m_{K^*} > 50$
(vii)	< 100	$ M(\pi^+\pi^-)_{rec} - m_{J/\psi} > 30$ $ M(K^\pm\pi_1^0) - m_{K^*} > 20$
(viii)	< 100	$ M(\pi^+\pi^-)_{rec} - m_{J/\psi} > 30$ $ M(\eta)_{rec} - m_{J/\psi} > 30$
(ix)	< 100	$ M(\pi^+\pi^-)_{rec} - m_{J/\psi} > 30$ $ M(K_S^0\pi_1^0) - m_{K^*} > 50$ $ M(K^\pm\pi_1^0) - m_{K^*} > 50$
(x)	< 50	$ M(\pi^0\pi^0)_{rec} - m_{J/\psi} > 30$ $ M(p\pi_1^0) - m_{\Delta(1232)^+} > 10$ $ M(p\pi_1^0) - m_{\Sigma^+} > 30$ $ M(\pi^0\pi^0\pi^0) - m_\eta > 25$

(denoted by N), is limited depending on the final state (see Table I). Additional vetoes in the $\pi^0\pi^0$, $\pi^+\pi^-$ and η recoil masses, as listed in Table I, are applied to suppress background from $\psi(3686) \rightarrow (\pi^0\pi^0, \pi^+\pi^-, \eta) J/\psi$. Since the π^0 from the decay $\psi(3686) \rightarrow \pi^0 h_c$ (denoted by π_1^0 and identified among all π^0 candidates by its energy being closest to the expected) should not create any structure together with other final state particles. Therefore, additional vetoes are applied to suppress background from $\omega \rightarrow \pi^+\pi^-\pi^0$, $\eta \rightarrow \pi^+\pi^-\pi^0$, $\eta \rightarrow \pi^0\pi^0\pi^0$, $K^{*\pm} \rightarrow \pi^0 K^\pm$, $\Delta(1232)^+ \rightarrow p\pi^0$ and $\Sigma^+ \rightarrow p\pi^0$ as given in Table I. The mass windows for these vetoes and for the χ^2 criterion are optimized simultaneously for each channel using the figure of merit of $S/\sqrt{S+B}$ and are listed in Table I. Here, S denotes the number of signal events,

obtained from signal MC, which is scaled to the branching fraction as determined in this analysis. Therefore, the unoptimized selection criteria were used in a first iteration to obtain a preliminary branching fraction (or upper limit). This preliminary result is then fed into the next iteration of optimization until the procedure converges within the uncertainties. The number of background events B is obtained from the $\psi(3686)$ inclusive MC and scaled to the expected number of events. Figure 1 shows the obtained invariant mass distributions of the different decay modes. After applying all selection criteria, the remaining background originates mostly from the non-resonant production of the same final state particles as the signal and thus cannot be suppressed further.

IV. Determination of Branching Fractions

To determine the number of signal events N_{h_c} , an unbinned maximum likelihood fit to the invariant mass spectra of the particles to reconstruct the h_c is performed as shown in Fig. 1. In each fit, the signal contribution is described by a Breit-Wigner function convoluted with a detector resolution function as given in Ref. [23]. Here, the mass and width of h_c in the Breit-Wigner function are fixed to their world average values [11], and the parameters in the resolution function are determined with the signal MC simulation. The background shape is described by an ARGUS function [24], where the threshold parameter of the ARGUS function is fixed to the kinematical threshold of 3551 MeV/ c^2 . In case of the modes $h_c \rightarrow K^+K^-\pi^+\pi^-\pi^0$ and $h_c \rightarrow \pi^+\pi^-\pi^0\eta$, additional peaking background from the processes $h_c \rightarrow \gamma\eta_c$, $\eta_c \rightarrow K^+K^-\pi^+\pi^-$ and $\eta_c \rightarrow \pi^+\pi^-\eta$ is included and scaled to the expected number of events based on the world average values. The resulting branching fractions are determined by:

$$\mathcal{B}(h_c \rightarrow X) \cdot \mathcal{B}(\psi(3686) \rightarrow \pi^0 h_c) = \frac{N_{h_c}}{N_{\psi(3686)} \cdot \prod_i \mathcal{B}_i \cdot \varepsilon}. \quad (1)$$

Here $\mathcal{B}(h_c \rightarrow X)$ denotes the branching fraction of the h_c meson decaying to final state X , the branching fraction of $\psi(3686) \rightarrow \pi^0 h_c$ is given by $\mathcal{B}(\psi(3686) \rightarrow \pi^0 h_c) = (8.6 \pm 1.3) \times 10^{-4}$ [11]. The number of $\psi(3686)$ events is given by $N_{\psi(3686)} = (448.1 \pm 2.9) \times 10^6$ [14]. And $\prod_i \mathcal{B}_i$ is the product of branching fractions of the decaying particles like $\mathcal{B}(\pi^0 \rightarrow \gamma\gamma)$, $\mathcal{B}(\eta \rightarrow \gamma\gamma)$ and $\mathcal{B}(K_S^0 \rightarrow \pi^+\pi^-)$ taken from [11]. The efficiency ε is obtained from signal MC simulations and N_{h_c} is the number of signal events obtained by the fit. In order to determine $\mathcal{B}(h_c \rightarrow X)$, the product branching fraction is divided by $\mathcal{B}(\psi(3686) \rightarrow \pi^0 h_c)$. Both values, the product branching fraction and the h_c decay branching fraction are listed in Table II.

In case no significant signal contribution is observed for the modes (iv)-(x), upper limits on the branching fractions are determined by the Bayesian approach [25]. To obtain the likelihood distribution, the signal yield is scanned using the fit function described earlier. Sys-

Table II. Overview of the branching fractions and upper limits obtained in this analysis for decay processes of the h_c meson. The first uncertainty shown is the statistical and the second the systematical uncertainty of the measurement method which includes the uncertainty that arises due to the use of external branching fractions.

Mode	X	N_{h_c}	ε (%)	$\mathcal{B}(\psi(3686) \rightarrow \pi^0 h_c) \times \mathcal{B}(h_c \rightarrow X)$	$\mathcal{B}(h_c \rightarrow X)$
(i)	$K^+ K^- \pi^+ \pi^- \pi^0$	80 ± 15	6.5	$(2.8 \pm 0.5 \pm 0.3) \times 10^{-6}$	$(3.3 \pm 0.6 \pm 0.6) \times 10^{-3}$
(ii)	$\pi^+ \pi^- \pi^0 \eta$	35 ± 9	3.3	$(6.2 \pm 1.6 \pm 0.7) \times 10^{-6}$	$(7.2 \pm 1.8 \pm 1.3) \times 10^{-3}$
		< 50.0		$< 1.5 \times 10^{-5}$	$< 1.8 \times 10^{-2}$
(iii)	$K_S^0 K^\pm \pi^\mp \pi^+ \pi^-$	41 ± 13	5.5	$(2.4 \pm 0.7 \pm 0.3) \times 10^{-6}$	$(2.8 \pm 0.9 \pm 0.5) \times 10^{-3}$
		< 65.3		$< 3.9 \times 10^{-6}$	$< 4.7 \times 10^{-3}$
(iv)	$K^+ K^- \pi^0$	< 20.1	9.8	$< 4.8 \times 10^{-7}$	$< 5.8 \times 10^{-4}$
(v)	$K^+ K^- \eta$	< 18.5	14.3	$< 7.5 \times 10^{-7}$	$< 9.1 \times 10^{-4}$
(vi)	$K^+ K^- \pi^+ \pi^- \eta$	< 24.1	6.9	$< 2.0 \times 10^{-6}$	$< 2.5 \times 10^{-3}$
(vii)	$2(K^+ K^-) \pi^0$	< 11.7	6.7	$< 2.1 \times 10^{-7}$	$< 2.5 \times 10^{-4}$
(viii)	$K^+ K^- \pi^0 \eta$	< 20.2	6.3	$< 1.8 \times 10^{-6}$	$< 2.2 \times 10^{-3}$
(ix)	$K_S^0 K^\pm \pi^\mp$	< 17.4	14.4	$< 4.8 \times 10^{-7}$	$< 5.7 \times 10^{-4}$
(x)	$p \bar{p} \pi^0 \pi^0$	< 11.8	8.7	$< 4.4 \times 10^{-7}$	$< 5.2 \times 10^{-4}$

tematic uncertainties are considered by smearing the obtained likelihood curve with a Gaussian function with the width of the systematic uncertainty of the respective decay mode. The upper limit at a confidence level of 90% is finally obtained by:

$$0.9 = \frac{\int_0^{N_{h_c}^{up}} dN \mathcal{L}(N)}{\int_0^\infty dN \mathcal{L}(N)}. \quad (2)$$

The upper limit on the number of observed events $N_{h_c}^{up}$ is determined by integrating the smeared likelihood function $\mathcal{L}(N)$ up to the value $N_{h_c}^{up}$, which corresponds to 90% of the integral. The results are listed in Table II.

Among the ten final states, the decay $h_c \rightarrow K^+ K^- \pi^+ \pi^- \pi^0$ is observed with a statistical significance of 6σ and evidences for the decays $h_c \rightarrow \pi^+ \pi^- \pi^0 \eta$ and $h_c \rightarrow K_S^0 K^\pm \pi^\mp \pi^+ \pi^-$ are found with statistical significances of 3.6σ and 3.8σ , respectively. The combined significance of the modes (iv)-(x) is determined to be 3.5σ . The statistical significance is determined by the likelihood ratio between a fit with and without signal component by taking the change in the number of fit parameters into account.

For the final state $K^+ K^- \pi^+ \pi^- \pi^0$ in the h_c decay, a search for intermediate resonances is performed to obtain information about underlying sub-processes. Despite the large background contamination, the signal content is determined by an unbinned maximum likelihood fit to the invariant $K^+ K^- \pi^+ \pi^- \pi^0$ mass in slices of masses of possible sub-systems. The resulting distributions are shown in the Fig. 2.

No firm conclusions about contributions of intermediate resonances can be drawn based only on the extracted projections with the present statistics. The $K\pi$ distribution shows a possible structure in the $K^*(892)$ region, which may signal the production of this resonance. In the invariant $K^\pm \pi^\mp \pi^0$ mass distribution there may be

a hint in the mass region of $1.9 - 2.0 \text{ GeV}/c^2$ for the production of an excited kaon, such as the $K_2^*(1980)$ or $K_2(1820)$. Conceivable sub-processes would then be $h_c \rightarrow (K^*(892)/K_{0,2}^*(1430)) (K_2(1820)/K_2^*(1980))$. As shown in this analysis, evidence for the decay $h_c \rightarrow K_S^0 K^\pm \pi^\mp \pi^+ \pi^-$ has been found.

V. Systematic Uncertainties

The sources of systematic uncertainties for the branching fractions include tracking, PID, selection, uncertainties caused by the signal fitting procedure and efficiency determination, and they are explained in the following. All the systematic uncertainties are summarized in Table III. The overall systematic uncertainty for the product branching fraction $\mathcal{B}(\psi(3686) \rightarrow \pi^0 h_c) \times \mathcal{B}(h_c \rightarrow X)$ is obtained by summing all individual components (from column two to six of Table III) in quadrature. An additional systematic uncertainty of $\Delta_{ext} = 15.1\%$ is added in quadrature due to the branching fraction of $\psi(3686) \rightarrow \pi^0 h_c$ used in the calculation of branching fractions of $\mathcal{B}(h_c \rightarrow X)$.

The uncertainties of the tracking efficiency are estimated using $J/\psi \rightarrow p \bar{p} \pi^+ \pi^-$ and $e^+ e^- \rightarrow \pi^+ \pi^- K^+ K^-$ control samples [26, 27]. The resulting uncertainties are determined to be 1% for each participating charged pion, kaon, proton, and antiproton, of a particular final state. The uncertainties due to PID are studied with control samples $e^+ e^- \rightarrow \pi^+ \pi^- K^+ K^-$ and $e^+ e^- \rightarrow p \bar{p} \pi^0$ and are estimated to be 1% for each participating pion, kaon, proton and antiproton [27, 28]. The uncertainty due to photon reconstruction is estimated to be 1% per photon based on studies of the reference channel $J/\psi \rightarrow \rho^0 \pi^0$ [29]. The uncertainties due to π^0 , η and K_S^0 reconstruction are studied by using the reference processes $J/\psi \rightarrow \pi^+ \pi^- \pi^0$, $J/\psi \rightarrow \eta p \bar{p}$ and $J/\psi \rightarrow K^{*\pm}(892) K^\mp$, $K^{*\pm}(892) \rightarrow K_S^0 \pi^\pm$ and are estimated to be 1% per π^0 and η [29] and 1.2% per K_S^0 [30]. For example in case of final state (i), two pions, two

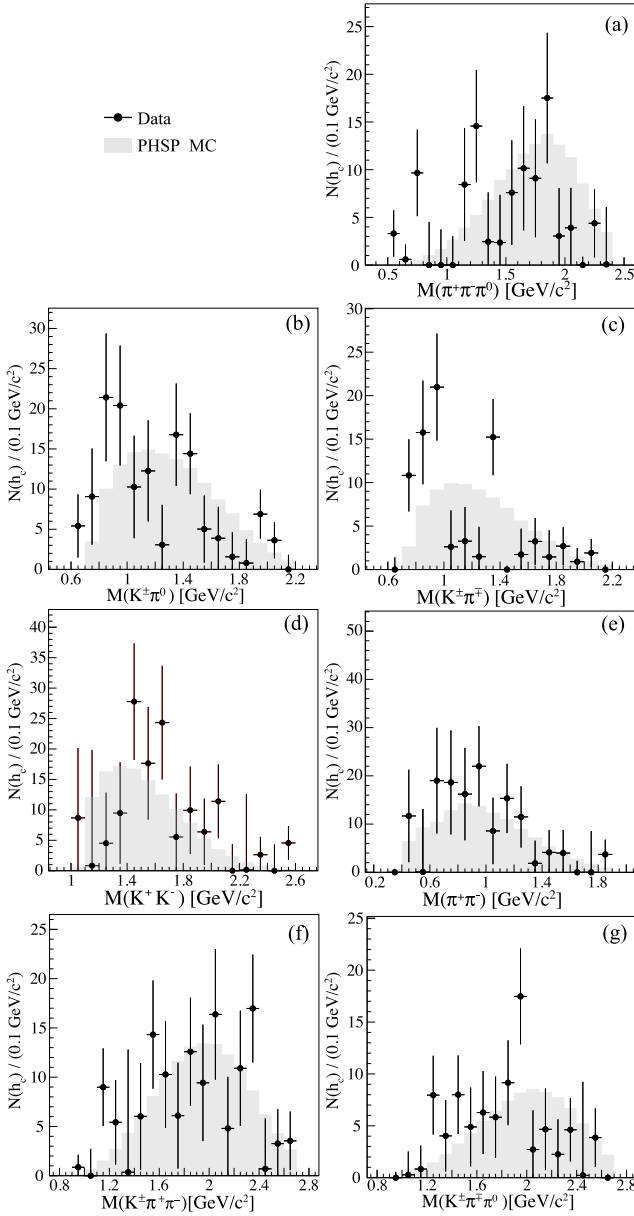


Figure 2. Signal yield obtained from an unbinned maximum-likelihood fit to the invariant $K^+K^-\pi^+\pi^-\pi^0$ mass in slices of the invariant $\pi^+\pi^-\pi^0$ (a), $K^\pm\pi^0$ (b), $K^\pm\pi^\mp$ (c), K^+K^- (d), $\pi^+\pi^-$ (e), $K^\pm\pi^+\pi^-$ (f) and $K^\pm\pi^\mp\pi^0$ (g) mass. Black dots denote the signal yield determined from data. The grey shaded histogram shows the PHSP distribution obtained from MC which is scaled to the integral of signal yield.

kaons and four photons reconstructed as π^0 are involved. This gives the following contributions to the systematic uncertainty: 4% (1% per track) due to PID, 4% (1% per track) due to track reconstruction, 4% due to photon reconstruction (1% per photon) and additional 2% for π^0 reconstruction (1% for each π^0). The total uncertainty due to PID and event reconstruction is given for each final state in the second column of Table III.

The systematic uncertainty due to the selection criteria

is determined by varying the nominal selection criteria. For each mass window requirement, the nominal value of the criterion is varied by $\pm 10 \text{ MeV}/c^2$ in increments of $\pm 0.5 \text{ MeV}/c^2$. The maximum deviation from the nominal branching fraction is quoted as a systematic uncertainty as given in column three of Table III.

The uncertainties associated with the kinematic fit are determined by comparing the efficiencies with and without the helix parameter correction. For charged particles, differences in the χ^2 distributions of the kinematic fit between data and MC have been studied by using a control sample $J/\psi \rightarrow \phi f_0(980)$, $\phi \rightarrow K^+K^-$, $f_0(980) \rightarrow \pi^+\pi^-$, which ensures high statistics and purity [31]. The helix parameters of the corresponding tracks are corrected accordingly [31]. The difference between the result determined with and without this correction applied are assigned as systematic uncertainty of the kinematic fit.

The systematic uncertainty due to the physics model and the efficiency used to simulate signal MC arises from the limited knowledge of intermediate states in the h_c decay. Therefore have MC samples been generated including additional intermediate states and the results are compared with those of the nominal phase space sample. The systematic uncertainty of the fit results from the choice of background parametrization is determined by using a second order Chebychev polynomial. In case of a peaking background, the uncertainty of the branching fraction (e.g. $\mathcal{B}(h_c \rightarrow \pi^+\pi^-K^+K^-) = (6.9 \pm 1.1) \times 10^{-3}$) [11] has been used to determine the uncertainty of the peaking background. This uncertainty contributes 1.2% in case of $h_c \rightarrow K^+K^-\pi^+\pi^-\pi^0$ and 2% in $h_c \rightarrow \pi^+\pi^-\pi^0\eta$, respectively. Another contribution to the systematic uncertainty of the fit is caused by the limited range of the invariant mass in which the fit is applied. Therefore, the fit range is extended from $3.50 - 3.55 \text{ GeV}/c^2$ to $3.40 - 3.65 \text{ GeV}/c^2$, and the difference of the branching fraction result is used as a systematic uncertainty. Further uncertainties arise from the parametrization of the resolution distributions. Instead of using the default parametrization, a Crystal Ball distribution has been used. The uncertainty arising from the number of $\psi(3686)$ events is 0.7% [14].

VI. Summary

In this analysis, ten final states of the h_c decays have been searched for using a data sample of $(448.1 \pm 2.9) \times 10^6$ $\psi(3686)$ events collected at BESIII. The decay $h_c \rightarrow K^+K^-\pi^+\pi^-\pi^0$ is observed for the first time. Furthermore, evidence for the decays $h_c \rightarrow \pi^+\pi^-\pi^0\eta$ and $h_c \rightarrow K_S^0 K^\pm \pi^\mp \pi^+ \pi^-$ are found with statistical significances of 3.6σ and 3.8σ , respectively. The combined significance of the modes (iv)-(x) is determined to be 3.5σ . Upper limits are determined in case there was no signal observed. The measured branching fractions and upper limits at 90% confidence level are listed in Table II.

Summing up the branching fractions obtained in this analysis, shows that these decays contribute at a level of $\sim 1.3\%$ to all decays and contribute at the same level

Table III. Summary of systematic uncertainties. Here $\Delta_{\mathcal{B}\mathcal{B}} = \sqrt{\sum_i \Delta_i^2}$ is the systematic uncertainty for $\mathcal{B}(\psi(3686) \rightarrow \pi^0 h_c) \times \mathcal{B}(h_c \rightarrow X)$ and $\Delta_{\mathcal{B}} = \sqrt{\sum_i \Delta_i^2 + \Delta_{ext}^2}$ is that for $\mathcal{B}(h_c \rightarrow X)$. Δ_i represents the individual uncertainties given in columns two to six and $\Delta_{ext}=15.1\%$ is an additional uncertainty for $\mathcal{B}(h_c \rightarrow X)$ due to the external uncertainty of $\mathcal{B}(\psi(3686) \rightarrow \pi^0 h_c)$ [11]. All values are given in %.

Mode	PID, Reco.	Sele- ction	Kin. Fit	Eff.	Fit	$\Delta_{\mathcal{B}\mathcal{B}}$	$\Delta_{\mathcal{B}}$
(i)	7.2	5.0	1.5	5.1	2.7	10.6	18.4
(ii)	7.0	4.4	2.1	6.3	2.8	11.0	18.7
(iii)	8.9	3.9	3.9	5.3	4.0	12.4	19.5
(iv)	5.3	3.7	1.9	4.1	3.8	8.8	17.5
(v)	5.1	2.0	1.9	3.7	3.4	7.7	16.9
(vi)	7.1	4.1	1.6	3.4	4.7	10.2	18.2
(vii)	7.2	4.7	2.3	5.2	3.7	10.6	18.5
(viii)	7.0	3.7	2.0	4.5	4.0	10.1	18.2
(ix)	6.2	3.3	2.1	4.0	3.4	9.0	17.6
(x)	7.3	6.0	2.7	4.9	3.3	11.5	19.0

as the previously observed decays $h_c \rightarrow 2(\pi^+\pi^-)\pi^0$ and $h_c \rightarrow p\bar{p}\pi^+\pi^-$ [12]. After the previous observations of multi-pionic decays [12], this is the first observation of the h_c decaying to mesons carrying strangeness. This observation adds another decay mode to the few observed hadronic decays of the h_c and the calculated upper limits further rule out strong contributions of other promising decay channels. These measurements provide input to theoretical models in order to improve their predictions in the future. Finally, it is still unclear if the hadronic decays width of the h_c is of the same order as the radiative decay width predicted in [2], or if the radiative decays

dominate. Although many final states have been investigated in this analysis, using the largest available data set of resonantly produced $\psi(3686)$ events, future experimental measurements of higher precision together with improved theoretical calculations can further contribute to answering these questions [32].

VII. Acknowledgments

The BESIII collaboration thanks the staff of BEPCII and the IHEP computing center for their strong support. This work is supported in part by National Key Basic Research Program of China under Contract No. 2015CB856700; National Natural Science Foundation of China (NSFC) under Contracts Nos. 11625523, 11635010, 11735014, 11822506, 11835012; the Chinese Academy of Sciences (CAS) Large-Scale Scientific Facility Program; Joint Large-Scale Scientific Facility Funds of the NSFC and CAS under Contracts Nos. U1532257, U1532258, U1732263, U1832207; CAS Key Research Program of Frontier Sciences under Contracts Nos. QYZDJ-SSW-SLH003, QYZDJ-SSW-SLH040; 100 Talents Program of CAS; INPAC and Shanghai Key Laboratory for Particle Physics and Cosmology; ERC under Contract No. 758462; German Research Foundation DFG under Contracts Nos. Collaborative Research Center CRC 1044, FOR 2359; Istituto Nazionale di Fisica Nucleare, Italy; Ministry of Development of Turkey under Contract No. DPT2006K-120470; National Science and Technology fund; STFC (United Kingdom); The Knut and Alice Wallenberg Foundation (Sweden) under Contract No. 2016.0157; The Royal Society, UK under Contracts Nos. DH140054, DH160214; The Swedish Research Council; U. S. Department of Energy under Contracts Nos. DE-FG02-05ER41374, DE-SC-0010118, DE-SC-0012069; University of Groningen (RuG) and the Helmholtzzentrum für Schwerionenforschung GmbH (GSI), Darmstadt.

-
- [1] F. Renard, Phys. Lett. B **65**, 157 (1976).
 - [2] G. T. Bodwin, E. Braaten, and G. P. Lepage, Phys. Rev. D **46**, R1914 (1992).
 - [3] V. Novikov *et al.*, Phys. Rep. **41**, 1 (1978).
 - [4] Y.-P. Kuang, S. F. Tuan, and T.-M. Yan, Phys. Rev. D **37**, 1210 (1988).
 - [5] G. Dissertori, I. Knowles, and M. Schmelling, ISBN: 9780199566419 International Series of Monographs on Physics (2009).
 - [6] P. Rubin *et al.* (CLEO Collaboration), Phys. Rev. D **72**, 092004 (2005).
 - [7] J. L. Rosner *et al.* (CLEO Collaboration), Phys. Rev. Lett. **95**, 102003 (2005).
 - [8] M. Andreotti *et al.* (Fermilab E835 Collaboration), Phys. Rev. D **72**, 032001 (2005).
 - [9] S. Dobbs *et al.* (CLEO Collaboration), Phys. Rev. Lett. **101**, 182003 (2008).
 - [10] M. Ablikim *et al.* (BESIII Collaboration), Phys. Rev. Lett. **104**, 132002 (2010).
 - [11] P. A. Zyla *et al.* (Particle Data Group), Review of Particle Physics, Progress of Theoretical and Experimental Physics **2020**, 10.1093/ptep/ptaa104 (2020), 083C01.
 - [12] M. Ablikim *et al.* (BESIII Collaboration), Phys. Rev. D **99**, 072008 (2019).
 - [13] G. S. Adams *et al.* (CLEO Collaboration), Phys. Rev. D **80**, 051106 (2009).
 - [14] M. Ablikim *et al.* (BESIII Collaboration), Chin. Phys. C **42**, 023001 (2018).
 - [15] M. Ablikim *et al.* (BESIII Collaboration), Nucl. Instrum. Methods Phys. A **614**, 345 (2010).
 - [16] C. Yu *et al.*, in Proceedings of IPAC2016, Busan, Korea, 1014 (2016).
 - [17] D. J. Lange, Nucl. Instrum. Methods Phys. A **462**, 152 (2001).
 - [18] R. G. Ping, Chin. Phys. C **32**, 599 (2008).
 - [19] S. Jadach, B. F. L. Ward, and Z. Wař, Phys. Rev. D **63**, 113009 (2001).
 - [20] S. Jadach, B. F. L. Ward, and Z. Wař, Comput. Phys. Commun. **130**, 260 (2000).

- [21] C. Patrignani *et al.* (Particle Data Group), Review of Particle Physics, Chin. Phys. C **40**, 100001 (2016).
- [22] J. C. Chen, G. S. Huang, X. R. Qi, D. H. Zhang, and Y. S. Zhu, Phys. Rev. D **62**, 034003 (2000).
- [23] S. Das, arXiv:1603.08591 [hep-ex].
- [24] H. Albrecht *et al.* (ARGUS Collaboration), Phys. Lett. B **340**, 217 (1994).
- [25] L. Demortier, Proceedings of the Advanced Statistical Techniques in Particle Physics **0203181**, 145 (2002).
- [26] W. L. Yuan *et al.*, Chin. Phys. C **40**, 026201 (2016).
- [27] M. Ablikim *et al.* (BESIII Collaboration), Phys. Rev. D **99**, 091103 (2019).
- [28] M. Ablikim *et al.* (BESIII Collaboration), Phys. Rev. D **86**, 092009 (2012).
- [29] M. Ablikim *et al.* (BESIII Collaboration), Phys. Rev. D **81**, 052005 (2010).
- [30] M. Ablikim *et al.* (BESIII Collaboration), Phys. Rev. D **99**, 032002 (2019).
- [31] M. Ablikim *et al.* (BESIII Collaboration), Phys. Rev. D **87**, 012002 (2013).
- [32] M. Ablikim *et al.* (BESIII Collaboration), Chin. Phys. C **44**, 040001 (2020).